



OPEN ACCESS

EDITED BY

Kelly Schultz,
Lehigh University, United States

REVIEWED BY

Daniele Tammaro,
University of Naples Federico II, Italy
Wylie Ahmed,
California State University, Fullerton,
United States

*CORRESPONDENCE

Shinji Tamano,
✉ tamano.shinji@nitech.ac.jp

RECEIVED 06 October 2023

ACCEPTED 29 November 2023

PUBLISHED 14 December 2023

CITATION

Muto M, Kikuchi K, Yoshino T, Muraoka A, Iwata S, Nakamura M, Osuka S and Tamano S (2023), Rheological characterization of human follicular fluid under shear and extensional stress conditions.
Front. Phys. 11:1308322.
doi: 10.3389/fphy.2023.1308322

COPYRIGHT

© 2023 Muto, Kikuchi, Yoshino, Muraoka, Iwata, Nakamura, Osuka and Tamano. This is an open-access article distributed under the terms of the [Creative Commons Attribution License \(CC BY\)](https://creativecommons.org/licenses/by/4.0/). The use, distribution or reproduction in other forums is permitted, provided the original author(s) and the copyright owner(s) are credited and that the original publication in this journal is cited, in accordance with accepted academic practice. No use, distribution or reproduction is permitted which does not comply with these terms.

Rheological characterization of human follicular fluid under shear and extensional stress conditions

Masakazu Muto¹, Keigo Kikuchi¹, Tatsuya Yoshino¹,
Ayako Muraoka², Shuichi Iwata³, Masanori Nakamura¹,
Satoko Osuka² and Shinji Tamano^{1*}

¹Department of Mechanical Engineering, Nagoya Institute of Technology, Nagoya, Japan, ²Department of Obstetrics and Gynecology, Graduate School of Medicine, Nagoya University, Nagoya, Japan, ³Department of Chemical Engineering, Nagoya Institute of Technology, Nagoya, Japan

The rheology of human follicular fluid has been empirically evinced to be related to the reproductive health status of individuals, which supports its use as an indicator for improving the success rates of *in vitro* fertilization. However, there is a dearth of studies investigating the viscoelastic properties of human follicular fluid. Moreover, a comprehensive elucidation of the rheological properties of complex fluids necessitates the assessment of data regarding both shear and extensional viscosities. Nonetheless, to the best of our knowledge, the extant literature does not include reports on the behavior of follicular fluid under extensional conditions. Consequently, this study aimed to analyze the shear and extensional viscosities of human follicular fluid. Primarily, the impact of oocytes on the rheology of follicular fluid was evaluated by measuring the shear viscosity of this fluid using a high-resolution coaxial cylinder viscometer. The shear viscosity of follicular fluid exhibited marked differences depending on the presence or absence of oocytes. Subsequently, a measurement system that enables the handling of minute quantities of body fluid was developed to determine the extensional viscosity of follicular fluid, which contains albumin. A comparison of the acquired follicular fluid data with that of the protein solution containing albumin demonstrated that the follicular fluid alone displayed extensional behavior, whereas the protein solution did not. Therefore, it can be inferred that the protein solution is not its sole determinant, as other constituents of the fluid, such as peptides and cumulus cells, may determine its rheological properties. This observation was not attained through the conventional technique consisting in shear viscosity measurements.

KEYWORDS

human follicular fluid, rheology, complex fluid, shear viscosity, extensional viscosity, extensional viscometer

Abbreviations: ART, assisted reproductive technology; EC, elasto-capillary; IC, inertio-capillary; OVA, ovalbumin; PEO, polyethylene oxide; RBC, red blood cell; TVEC, terminal visco-elasto-capillary; VC, visco-capillary.

1 Introduction

In recent years, the prevalence of infertility treatment through assisted reproductive technology (ART) has significantly increased [1–3]. ART is a treatment strategy that artificially promotes pregnancy by culturing harvested gametes (oocytes and sperm) outside the body and includes intracytoplasmic sperm injection, *in vitro* fertilization, and embryo transfer. The pregnancy rate achieved through ART is approximately 30% per embryo transfer [3], being imperative to increase this success rate to alleviate the financial, physical, and emotional strain on infertile patients. To this end, the best oocytes must be obtained. The oocyte fertilization rate can be increased by selecting the best sperm for oocytes [4] and applying the oocyte activation method [5]. Another method is to analyze the results of time-lapse observation using artificial intelligence (AI) [6] to evaluate the development of oocytes until they become fertilized, although the efficacy of this method has not been proven. While the above procedures are performed before oocyte fertilization, even when fertilized oocytes are obtained, they are not always successful, and there is the possibility of miscarriage at the embryo transfer stage. To reduce this probability, some cells of the embryo are biopsied and tested for chromosomal aberrations using a next-generation sequencer [7]. However, this method has the disadvantage of being invasive because it requires a biopsy examination of the embryo. Thus, although these various methods are employed in ART, the most important factor in increasing the success rate of pregnancies recurring to ART is selecting the best oocytes at the initial stages.

Artificial fertilization through ART involves the aspiration of oocytes from mature follicles prior to ovulation. The human ovarian follicle consists of mural granulosa and theca cells on its outer surface [8] and encapsulates the oocyte, surrounded by cumulus cells and follicular fluid (Figure 1). The follicle is 150–400 μm in diameter and predominantly comprises 200–3,000 cumulus and mural granulosa cells [9–11], both of which are approximately 10–15 μm in diameter [12]. When an oocyte is aspirated, the follicular fluid that fills the follicle is collected as a secondary

sample. Follicular fluid is composed of substances derived from the blood, local secretions, and metabolism. It contains biochemical components such as hormones, enzymes, anticoagulants, electrolytes, active oxygen species, and antioxidants [13, 14]. Furthermore, the composition of the follicular fluid has been demonstrated to vary depending on the degree of oocyte maturation [10, 13, 14].

As oocyte maturation is associated with the balance in protein constituents of the follicular fluid, the rheological properties of this fluid are hypothesized to reflect the quality and fertility potential of oocytes; consequently, a quantitative rheological analysis would facilitate the selection of oocytes better suited for ART. Moreover, the rheological properties of the follicular fluid have been empirically evinced to be influenced by the medical condition of an individual regarding the degree of oocyte maturation at the time of fluid collection, such as age and stage of the menstrual cycle. Nevertheless, research on the rheology (delineation of the simple flow and deformation of complex fluids) properties of follicular fluid has been limited [15, 16]. A study quantitatively evaluated the shear viscosity-dependent characteristics of porcine, bovine, and human follicular fluids [15] using a cone-plate viscometer; the shear viscosity of human follicular fluid was 1–2 mPa s within the shear rate range of 75–750 s^{-1} , which is lower than those of porcine and bovine follicular fluids [15]. Furthermore, the shear viscosity of human follicular fluid exhibited a shear-thinning property, meaning that the shear viscosity decreased with an increasing shear rate [15]. Another study that assessed the shear viscosity of human follicular fluid and the maturation state of the sample using a B-type viscometer documented the absence of a relation between them [16]. However, the limited precision of the B-type viscometer used in the aforementioned study hindered the accurate detection of shear viscosity in the order of one-tenth of mPa s; this suggested that the viscosity measurement was unable to reflect differences in the shear viscosity of human follicular fluid attributable to distinct maturation states of the sample. Furthermore, the determination of the rheological properties of complex fluids necessitates the measurement of not only their shear

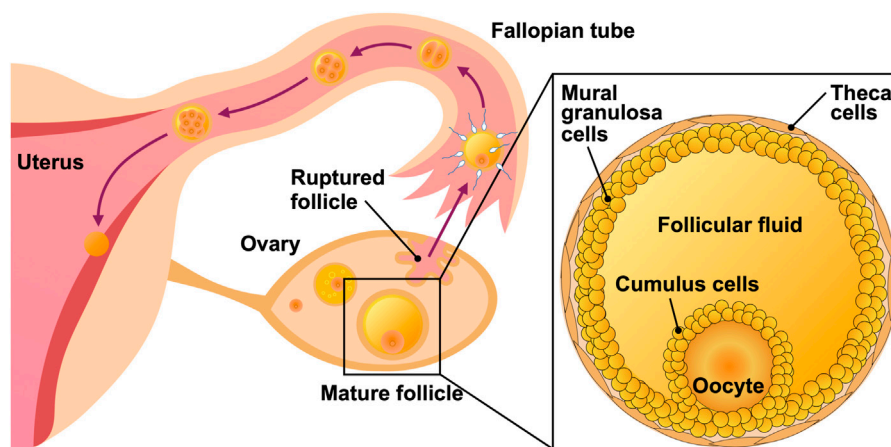


FIGURE 1

Illustration of the female reproductive system and human ovarian follicle. The follicle harbors mural granulosa and theca cells on its outer surface, and an oocyte surrounded by cumulus cells and follicular fluid.

viscosities but also extensional viscosities. Nonetheless, despite the documentation of the shear and extensional viscosities of other body fluids [17, 18], the behavior of human follicular fluid under extensional conditions (outside of a study using follicular fluid from chicken eggs [19]) remains unexplored to the best of our knowledge. In addition, the measurement of extensional viscosity of follicular fluid is challenging due to its extremely low viscoelasticity.

Thus, this study endeavored to assess the rheology of human follicular fluid using shear and extensional viscometry. The shear viscosity of the follicular fluid was measured using a coaxial cylinder viscometer. Moreover, the impact of internal structural modifications attributable to the removal of the cumulus, mural granulosa, and red blood cells (RBCs) on the shear viscosity of follicular fluid was examined. The association between the shear viscosity-based characteristics of follicular fluid and oocyte maturity was then delineated by analyzing shear viscosity data acquired from follicular fluid samples collected at different stages of oocyte development. The high sample variability and limited sample availability pose substantial challenges in surveying the rheological properties of follicular fluids. Although certain shear viscosity-measuring devices have overcome these challenges through technological advancements, current devices measuring extensional viscosity have not. Therefore, we also developed a novel apparatus for measuring extensional viscosity featuring disposable and replaceable components that come into contact with the sample, thereby mitigating the inadvertent risk of sample contamination. Furthermore, the device was designed to enable rheological measurements of minute amounts of sample, including those in the order of sub-milliliters. Additionally, the shear and extensional viscosities of pure water, protein solutions, and dilute polymer solutions were compared with those of follicular fluid. In general, human follicular fluid contains 58 ± 1.0 mg/mL of protein, of which 40 ± 1.9 mg/mL is albumin [20–22]; thus, the viscosity of this protein alone was also measured to evaluate the effect of its presence on the rheological properties of human follicular fluid. As the polymer in dilute polymer solutions, we used polyethylene oxide (PEO), which is often used to investigate the extensional viscosity properties of complex fluids [23–27].

2 Materials and methods

2.1 Materials

The bioethical review committees of the Nagoya Institute of Technology (approval no. 2022-7) and Nagoya University Hospital (approval no. 2022-0010) approved the experimentation and handling of the follicular fluid samples used in this study. Follicular fluid samples (1–10 mL) were collected via syringe aspiration from a cohort of seven Japanese women aged between 30 and 45 years. Since the cohort was small and only a limited dataset was available, some caution should be demonstrated when extrapolating the results of this study. Samples were sealed in conical tubes and stored in a refrigerated medicine showcase (MPR-S300H-PJ, PHC Co., Ltd.) at 4°C. Some samples collected at the Department of Obstetrics and Gynecology at the Nagoya University Hospital contained oocytes, whereas others did not. Oocytes, if detected in samples, were extracted with meticulous precision by medical

professionals, and the remaining samples that were deemed unnecessary were utilized for measurement purposes. Only samples with a minimum volume of 3 mL were subjected to measurements. As four to seven follicles could be collected from each individual, the sample size of follicular fluid per individual also ranged from four to seven.

Follicular fluid samples differed in color owing to the variation in RBC concentration (Figure 2). Samples were centrifuged at 10,000 rpm for 5 min using a MagFuge (Heathrow Scientific LLC), following which the pellet containing RBCs was discarded. The supernatant was collected using a micropipette and stored in a separate microtube in a refrigerated medicine showcase.

Pure water, protein, and dilute polymer solutions were prepared for analysis. Ovalbumin (OVA) (4 wt%; Fujifilm Wako Pure Chemical Corporation), predominant protein component of egg white, dissolved in phosphate-buffered saline (pH 7.1–7.3; Fujifilm Wako Pure Chemical Corporation) was used as the protein solution. OVA is a glycoprotein with a molecular weight of 45,000 and accounts for 54% of the egg white protein. Three different PEO (molecular weight = 1×10^6 g/mol; Sigma-Aldrich Inc.) solutions at the concentrations of 0.03, 0.05, and 0.1 wt% were formulated as diluted polymer solutions. The aforementioned PEO solutions were regarded as diluted polymer solutions below the overlap concentration $c^* = 0.17$ wt% [23].

2.2 Experimental setup for measuring shear viscosity

The shear viscosity of follicular fluid was measured using an experimental setup comprising a coaxial cylinder viscometer (ONRH-1B, Ohna Tech Inc.) and a temperature control system (Figure 3). The coaxial cylinder viscometer was coupled to an elastic-hinged bearing to facilitate highly accurate torque measurement. In this viscometer, the sample is placed between a bob and a cup that share a rotation axis, and the shear viscosity is obtained from the relation between the torque stress and the rotation speed of the cup [28, 29]. The steady-state speed ranged from 0.001 to 1,000 rpm, and the frequency ranged from 0.001 to 10 Hz. The outer diameter of the bob made of titanium was 19.36 mm, the inner diameter of the cup made of glass was 21.00 mm, and the gap width between them was 0.82 mm.

To maintain the temperature of the sample filling the cup of the viscometer, a temperature control system was constructed using both a small circulating cooler with a built-in thermostat (ZC-500 α , Zensui Co., Ltd.) and a throw-in pipe heater (LY-MAC103, As One Corporation). The heater was connected to the cooler, and water was circulated using a water pump (Rio+ 1100 60 Hz, Kamihata Fish Industry Co., Ltd.) to maintain the temperature in the chamber. Circulating water was drawn into the cooler by the pump, cooled, and returned to the thermostatic chamber. Circulating water was heated using a pipe heater inserted into the thermostatic chamber. By using this temperature control system, the shear viscosity was measured at the temperature of $25^\circ\text{C} \pm 0.5^\circ\text{C}$ in the torque sensor section. In the case of follicular fluid, measurements taken at body temperature (37°C) are preferred; however, the shear viscosity at 37°C is lower than that at 25°C and was not suitable for investigating rheological properties (see Supplementary Material).



FIGURE 2
Follicular fluid specimens sealed in conical tubes. Ovarian follicular fluid is conventionally yellow but turns red with increased concentration of red blood cells.

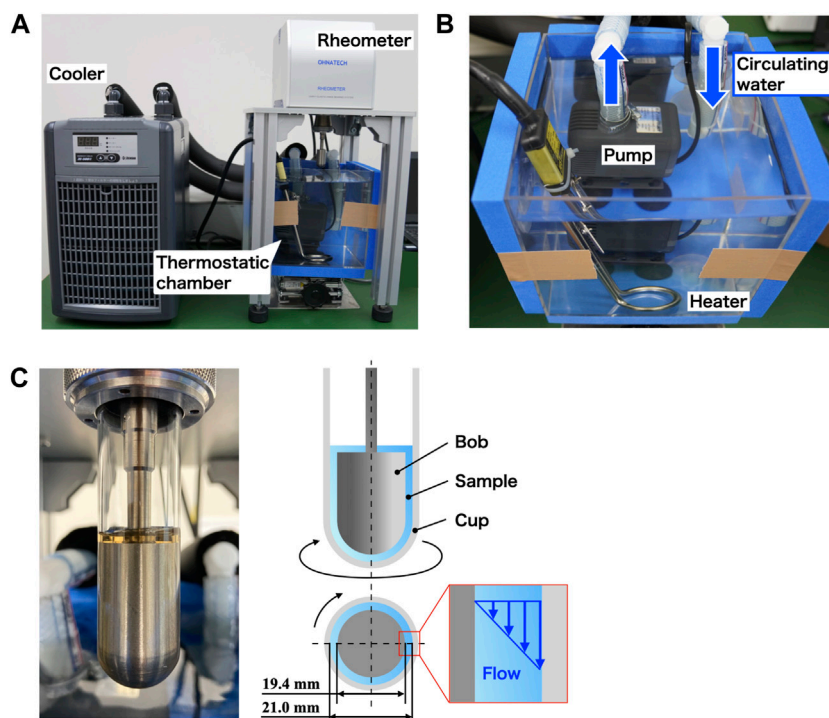


FIGURE 3
Experimental setup for measuring shear viscosity. (A) Photograph of the experimental setup consisting of (B) a thermostatic chamber with a temperature control system and (C) coaxial cylinder viscometer.

2.3 Experimental setup for measuring extensional viscosity

Figure 4 shows a photograph and schematic diagram of the experimental setup used to measure the extensional viscosities of the samples. This experiment employed a liquid dripping technique,

which enabled the evaluation of the extensional viscosity by measuring the diameter of the filament of a droplet suspended from a micro-nozzle [24, 25, 30]. Section 3.2 delineates the method for deriving the extensional viscosity from filament diameter data. The liquid dripping apparatus attached to a syringe pump (Pump 11 Elite, Harvard Apparatus Inc.) consisted of a 2.5 mL syringe

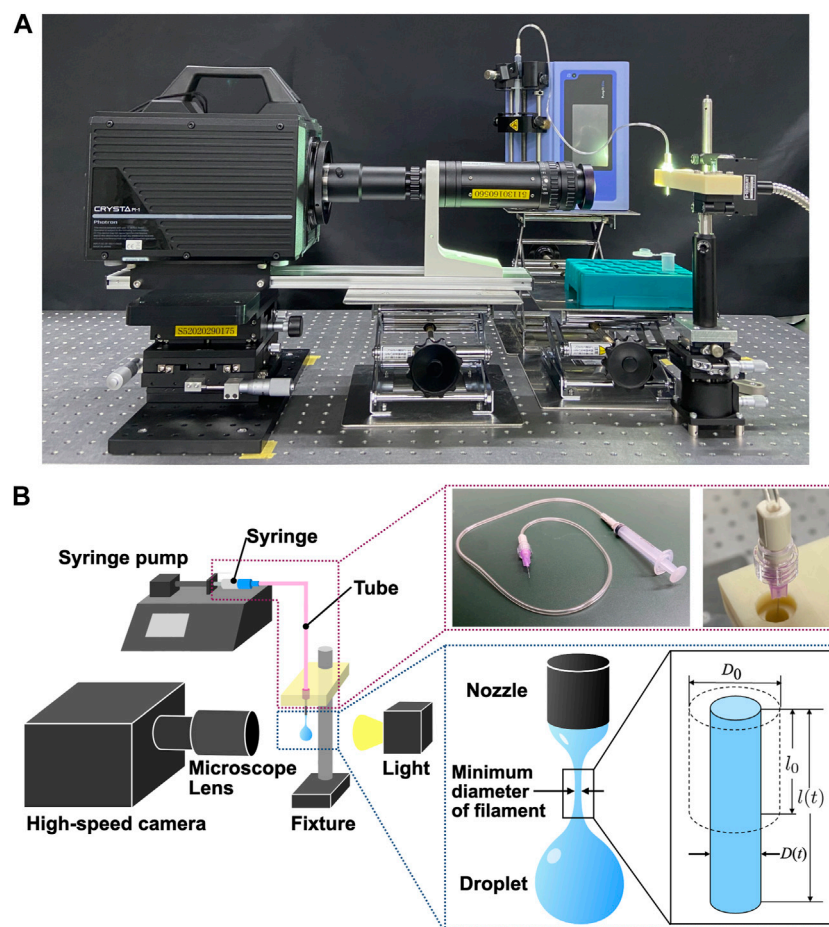


FIGURE 4

Experimental setup for measuring extensional viscosity employing a liquid dripping method [24, 25, 30]. (A) Photograph of the experimental setup. (B) Scheme of the experimental setup with photographs of specific components.

(Terumo syringe ss-02Sz, Terumo Corporation), 0.5 mL silicone tube (SF-ET0525L22, Terumo Corporation), and micro-nozzle with a 0.3 mm outer diameter (DPN-30G-1, Musashi Engineering Inc.), all of which were disposable and were replaced for each individual sample. The utilization of intricate parts facilitated measurements with a sampling volume of 3 mL or less. The measurements were conducted at room temperature (25 °C). Samples were allowed to drip from the micro-nozzle at a flow rate of 10 μ L/min.

A light source (UFLS-751-08W-UT, U-Technology Corporation) and a high-speed camera (CRYSTA PI-IP, Photron Co. Ltd.) coupled to a microscope lens at $\times 5$ magnification (Leica Z16APO, Leica Microsystems Ltd.) were used to capture the high-speed behavioral event of liquid filament thinning. The images were captured at a frame rate of 100,000 frames per second, a shutter speed of 1/100,000 s, and a maximum spatial resolution of 2.14 μ m/pix. Image analysis was performed using the programming language MATLAB (R2022b, Mathworks Ltd.) to enumerate the filament diameter required to calculate the filament extensional viscosity. The minimum diameter of the liquid filament in each image was computed by applying subpixel processing using a linear interpolation method [24] to the binarized images generated from the continuous-intensity images. Subpixel processing enabled us to analyze fast-varying diameters more accurately.

3 Results and discussion

3.1 Shear viscosity of follicular fluids

Follicular fluid samples were centrifuged prior to the experiment. Some samples retained their original yellow color after centrifugation, whereas others that were originally red in color turned yellow after centrifugation (Figures 5A, B). Colored images of the follicular fluids sealed in a plastic cell measuring 5 mm, 12 mm, and 18 mm in width, depth, and height, respectively, were captured using a single-lens reflex camera ($\alpha 7RIV$, Sony Corporation) fitted with a macro lens (FE 90 mm F2.8 Macro G OSS, Sony Corporation). Moreover, follicular fluid samples were observed under a microscope before and after centrifugation, which confirmed that the extant RBCs were removed after centrifugation; this elucidated that the original red color of certain samples changed to yellow because of RBC elimination. As granulosa cells can be removed through centrifugation at 100 g (approximately 2,500 rpm) for 10 min [31], centrifugation of samples at 10,000 rpm for 5 min appeared to partially but sufficiently remove granulosa cells.

Subsequently, the impact of centrifugation on the shear viscosity of samples was investigated (Figure 5C; sample size = 12). The

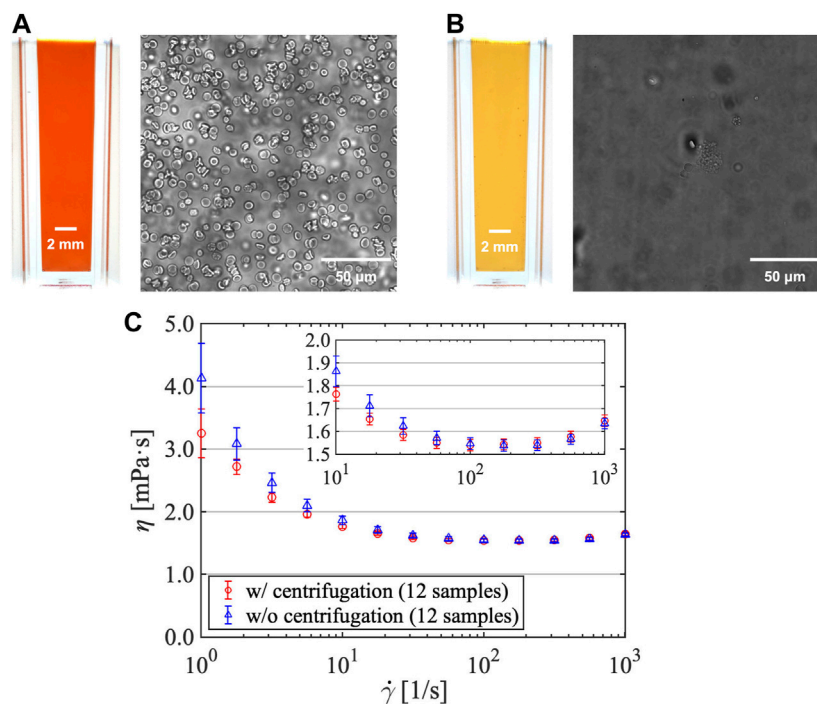


FIGURE 5 Follicular fluid color and red blood cell density (A) before and (B) after centrifugation. (C) Shear viscosity vs. shear rate for follicular fluids (subjected and not subjected to centrifugation).

measurement conditions were a steady shear viscosity under several shear rates without pre-shear. The shear rate was programmed to escalate from a low shear rate of 10^0 1/s to a high shear rate of 10^3 1/s, and then decline to a low shear rate, which was repeated three times. The shear viscosity of follicular fluids decreased with increasing shear rate, confirming that they possess shear-thinning properties similar to those reported in a previous study [15]. Moreover, the obtained values were approximately 1.5–2 mPa s in the shear rate range of 10^1 – 10^3 1/s, which were also similar to those obtained in a previous study [15]. As the respective error bars overlapped in the shear rate range of 10^0 – 10^3 1/s, we concluded that the presence of RBCs after centrifugation did not exert any effect on the shear viscosity of follicular fluids. Generally, in whole blood, shear viscosity increases with increasing concentration of RBCs in the plasma (low-viscosity Newtonian fluids) [32]. However, this effect was negligible in this study, indicating that the concentration of RBCs in follicular fluids was visibly minute. It should also be noted that the effect of RBCs on the extensional viscosity was not investigated in this study.

Figure 6 illustrates the relation between shear viscosity η and shear rate $\dot{\gamma}$ of pure water, OVA solution, dilute polymer solutions, and follicular fluids. The slight decrease and increase in the shear viscosity of water (Newtonian fluid) down to a shear rate of 10^0 1/s and up to a shear rate of 10^3 1/s, respectively, represent the measurement limits of the used coaxial cylinder viscometer. Note that the slight decrease and increase in the shear viscosity (down to a shear rate of 10^0 1/s and up to 10^3 1/s, respectively) represent the measurement limits of the viscometer, as pointed out by Ewoldt et al. [33]. The shear viscosity of dilute PEO solutions exhibited

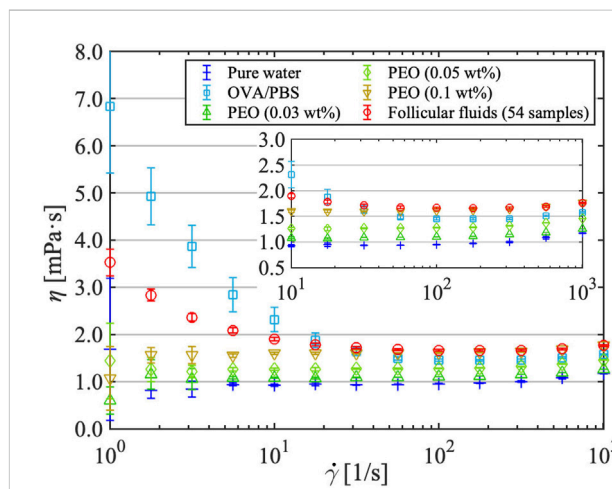


FIGURE 6 Shear viscosity vs. shear rate for pure water, protein (OVA/ phosphate-buffered saline) solution, dilute polymer (PEO) solutions, and follicular fluids. Error bars include both measurement- and sample-derived errors for follicular fluids and measurement-derived errors only for the other solutions.

Newtonian behavior, where the shear viscosity was independent of the shear rate. In contrast, the shear viscosities of OVA solution and follicular fluids displayed shear-thinning properties, where the shear viscosity decreased with increasing shear rate, indicating that they were non-Newtonian fluids. Fifty-four samples of follicular fluids were prepared for this study. The shear viscosity of the dilute

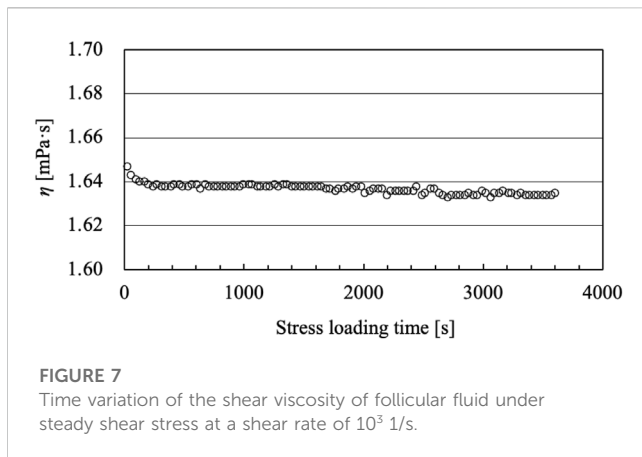


FIGURE 7
Time variation of the shear viscosity of follicular fluid under steady shear stress at a shear rate of 10^3 1/s.

polymer solutions used in this study was almost the same as that of water. It increased by approximately 0.2 mPa s with the slight increase in PEO concentration from 0.03 to 0.1 wt%, which is consistent with the results of a previous study [23], indicating high measurement accuracy. The shear viscosity of the OVA solution showed shear-thinning properties, consistent with the findings of a previous study on bovine serum albumin [34]. The shear viscosity of follicular fluids was relatively close to that of the OVA solution in the high shear rate range. Therefore, considering that the majority of proteins in the follicular fluid are OVA, the non-Newtonian property of the shear viscosity of follicular fluids might be predominantly attributable to the effect exerted by OVA.

When measuring the shear viscosity of follicular fluids (Figure 6), the shear rate increased and decreased three times in reciprocal cycles, and no significant hysteresis was observed in the process. This was also evident from the shear viscosity measurements at the constant high shear rate of 10^3 1/s (Figure 7). When the obstetrician/gynecologist collected oocytes and follicular fluids from the subjects, they used a lumen needle with a diameter of 0.8 mm (U5099-MM, 21G \times 300 mm, Hakko Co., Ltd.). The shear rate acting on the follicular fluids flowing through the needle is estimated to be the order of 10^3 1/s. Therefore, the extent of shear viscosity reduction upon application of a shear rate of 10^3 1/s to the follicular fluid for 1 h (3,600 s) was investigated. It was expected that high shear stress on follicular fluids would disrupt their internal structure and consequently affect shear viscosity. However, the shear viscosity of follicular fluids decreased by approximately 0.73% after experiencing a high shear rate of 10^3 1/s for 1 h, indicating little degradation. Therefore, although the follicular fluid contains various types of cells, it does not form structures, and the effect of degradation on shear viscosity due to shear stress is negligible.

The relation between the shear viscosity characteristics of follicular fluid and oocyte maturity was investigated. Here, information on oocyte maturity provided by the Department of Obstetrics and Gynecology of the Nagoya University Hospital and the corresponding shear viscosity data of follicular fluid samples were investigated. Cases in which the oocyte was present in the follicle were classified as “with oocyte,” and those in which the oocyte was absent from the follicle were classified as “without oocyte.” A comparison of the shear viscosities of follicular fluids with and without oocytes is shown in Figure 8. In this study, 16 and

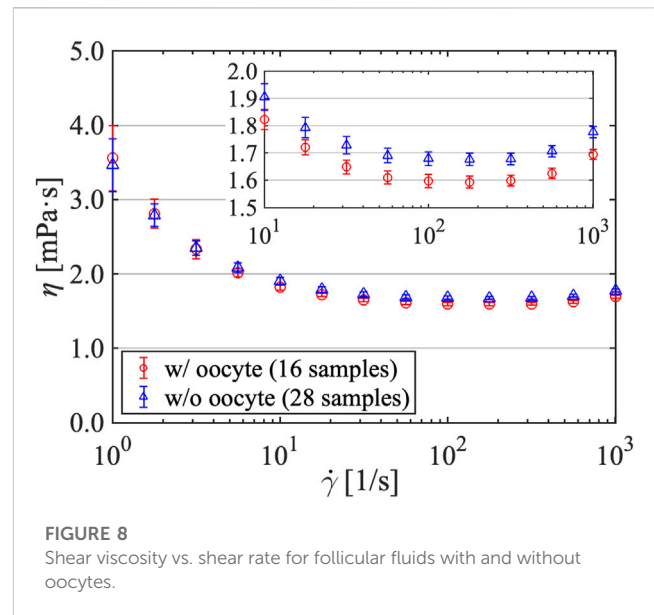


FIGURE 8
Shear viscosity vs. shear rate for follicular fluids with and without oocytes.

28 samples of follicular fluid with and without oocytes, respectively, were prepared. In the low shear rate range of 10^0 – 10^1 1/s, the shear viscosities of all cases were similar, and the error bars overlapped. Nevertheless, in the high shear rate range of 10^1 – 10^3 1/s, the shear viscosities of the two groups were different, and the error bars did not overlap. Furthermore, the high shear rate range induced a substantial difference of up to 0.1 mPa s between samples with and without oocytes. This suggests that the shear viscosity of follicular fluid differs depending on the presence or absence of oocytes. The protein and peptide composition of follicular fluid varies depending on the presence or absence of oocytes [20–22]; we speculate that this is a primary factor affecting our results. However, as we did not obtain biochemical data of the follicular fluids, we were unable to compare the composition of samples with and without oocytes, which prevents us from discussing the specific factors underlying the observed difference; this is a subject for future investigation.

3.2 Extensional viscosity of follicular fluids

The variability of data among follicular fluid samples was evidently minute for shear viscosity but large for extensional viscosity; thus, extensional viscosity data of only one follicular fluid sample, in which the extensional property appears, are presented in this section. The variability in our data on the extensional behavior of follicular fluid and OVA solutions have been described in the [Supplementary Material](#). Figure 9 shows an image time series of the extensional behavior of pure water, protein solution, dilute polymer solution, and follicular fluid captured using a high-speed camera. In the case of water, no liquid filament was formed; however, in the case of the protein solution, dilute polymer solution, and follicular fluid, the formed liquid filament with a cylindrical shape showed a uniaxial extension and gradually became thinner with time. It is well established that a filament is not formed in the case of water (Newtonian fluid) but is formed in the case of a PEO solution used as dilute polymer solution (non-Newtonian

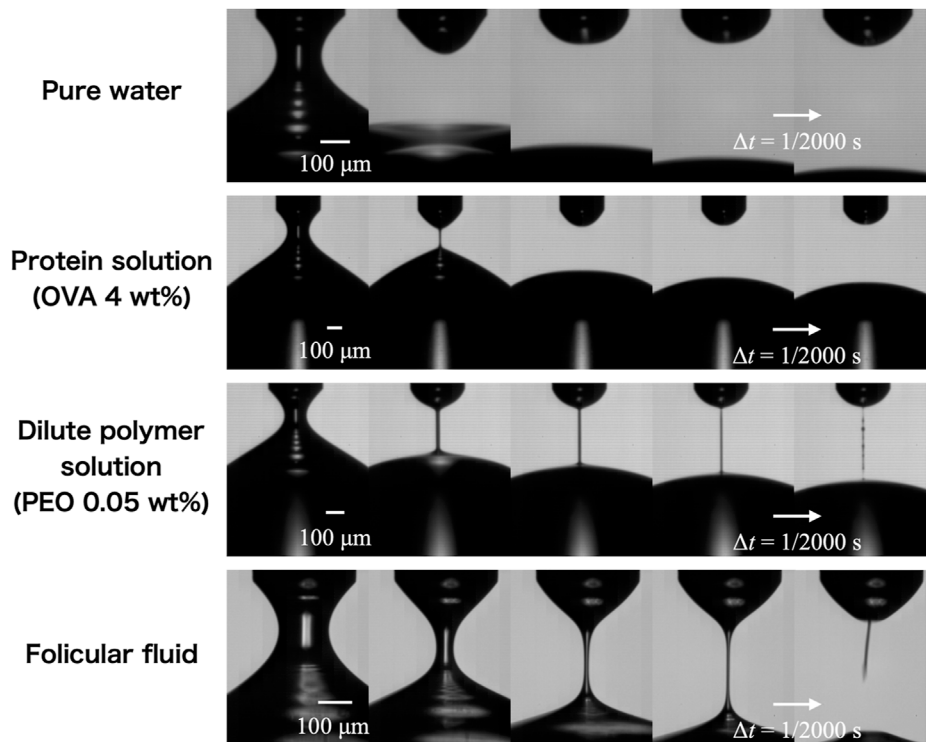


FIGURE 9

Temporal evolution of the extending liquid filament of pure water, protein (OVA/phosphate-buffered saline) solution, 0.05 wt% polymer (PEO) solution, and follicular fluid. The time interval shown from left to right is $\Delta t = 1/2,000$ s, while that of the actual photo is $1/100,000$ s.

fluid) [23–27]. Therefore, this suggests that the protein solution and follicular fluid that formed filaments are non-Newtonian fluids. Note that although the shear viscosity data for the PEO solution showed Newtonian behavior (Figure 6) because of the measurement limit of the viscometer, the filament behavior of the PEO solution indicates non-Newtonian fluids. To quantify the extensional behavior, we derived the extensional viscosity using the method described below.

Figure 10A shows a semi-logarithmic graph of the diameter ratio versus time for pure water, protein solution, diluted polymer solution, and follicular fluid. The diameter ratio is a dimensionless number obtained by normalizing the minimum diameter of the liquid filament at each time instant D to the outer diameter of the capillary nozzle D_0 . The horizontal axis represents the elapsed time t [ms], where $t = 0$ is the time at which $D/D_0 = 0.7$. The time evolution of the liquid filament of a viscoelastic fluid is mainly classified into three regimes: inertio-capillary (IC) or visco-capillary (VC), elasto-capillary (EC), and terminal visco-elasto-capillary (TVEC) regimes [27]. The EC regime is theoretically a perfect uniaxial extension, with an exponential decay of the diameter ratio D/D_0 with respect to time t , expressed as follows:

$$\frac{D}{D_0} \sim \exp\left[-\frac{(t - t_{EC})}{3\lambda_E}\right] \quad (1)$$

where t_{EC} is the onset time of the EC regime, that is, the time at which D/D_0 begins to decay exponentially with respect to time t , and λ_E is the extensional relaxation time. Newtonian fluids only have the

IC or VC regime, whereas viscoelastic fluids have EC and TVEC regimes that are further developed from the IC or VC regime. An inflection point exists as the slope of the diameter ratio changes during the transition from the IC or VC regime to the EC regime. As the TVEC regime is the moment when the extending liquid filament fails, data may not have been accurately acquired because of the low spatial resolution of the camera, and the TVEC regime was not confirmed for all data in this study. Therefore, only the diameter ratio data in the EC regime were used to calculate the extensional viscosity; the diameter ratio data in the TVEC regime were not used. Six measurements were conducted for each solution, and the error bars obtained from these six measurements are shown in Figure 10. The reproducibility of the extensional behavior was high in pure water, protein solutions, and dilute polymer solutions, confirming the reliability of this measurement system. In contrast, in the follicular fluid sample, two measurements showed extension and four did not, despite pertaining to the same sample. In other words, we obtained two measurement data with an EC regime and four without. As it was impossible to calculate the extensional viscosity for the data without the EC regime, only data with the EC regime were used for further analysis.

As shown in Figure 10A, the diameter ratios of pure water and protein solution did not exhibit an exponential decay trend with respect to time. Therefore, the protein solution was considered a Newtonian fluid with only the IC or VC regime, similar to water (Newtonian fluid). The extensional behavior of the protein solution in this measurement system was consistent with that reported in a

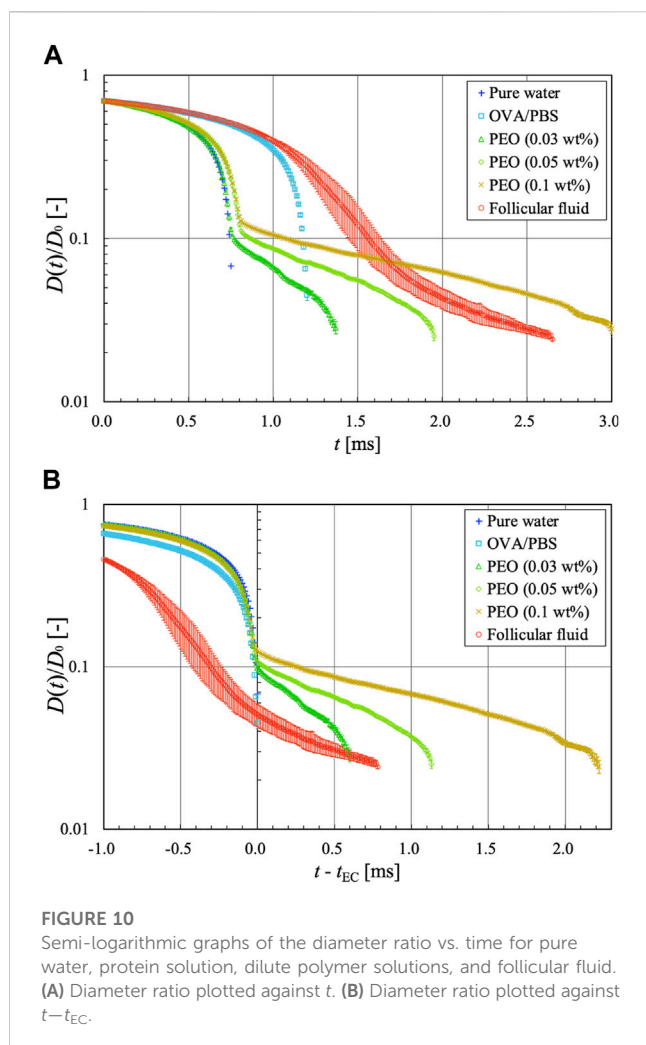


FIGURE 10
Semi-logarithmic graphs of the diameter ratio vs. time for pure water, protein solution, dilute polymer solutions, and follicular fluid. (A) Diameter ratio plotted against t . (B) Diameter ratio plotted against $t - t_{EC}$.

previous study [35]. Although the liquid filament of the protein solution extended uniaxially (Figure 9), the analytical results did not show a clear EC regime. It is possible that this measurement system does not clearly detect the extensional filament behavior of the protein solution owing to limitations in the spatio-temporal resolution. The proteins are generally surface-active molecules that affect interfacial behavior. Tammaro et al. [36] reported that proteins (such as BSA) can exhibit strong interfacial viscoelasticity at the protein surface layer when accompanied by bubble rupture dynamics. By contrast, Regev et al. [37] noted that the interfacial viscoelasticity for a protein surface layer of uniaxially extending filaments exerts a surface-stabilizing effect on the overall filament; this phenomenon is strongly dependent on the Peclet number, which is the ratio of the timescale of protein diffusion and the timescale of surface dilatation. Furthermore, in uniaxial extensional flows of proteins such as BSA, the Peclet number exceeds 1; thus the effect of interfacial viscoelasticity can be ignored [37]. Brust et al. [38] also noted that the effect of interfacial viscoelasticity is negligible in the uniaxial extensional flow of plasma protein solutions. In the present study, which deals with the uniaxial extensional flow of protein solutions using the LD method, the effect of interfacial viscoelasticity can be ignored because the Peclet number exceeds 1, as in previous studies [37, 38].

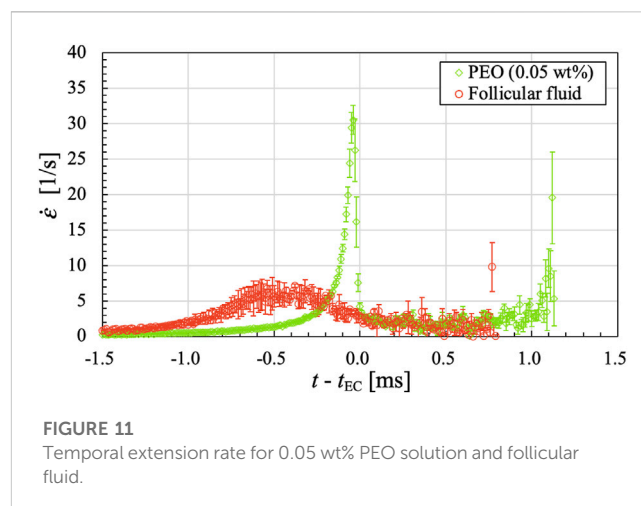


FIGURE 11
Temporal extension rate for 0.05 wt% PEO solution and follicular fluid.

In contrast, the dilute polymer solutions and follicular fluid showed an EC regime in which the diameter ratio decayed exponentially with time, confirming that they were viscoelastic fluids. We believe that human follicular fluid likely has elastic properties because it was confirmed (via an experimental investigation of its uniaxial extensional behavior) that the follicular fluid of chicken eggs possesses elastic properties [19]. The PEO solutions showed the same trend, which is consistent with the findings of a previous study [26], indicating that our measurement system is reliable. The diameter ratios of water and dilute polymer solutions showed the same curve up to the midpoint of the IC or VC regime, and the dilute polymer solutions further evolved over time to reach the EC regime. This is due to the influence of polymer chains dispersed in water, which impart rheological properties to water. Interestingly, this was also the observed relation between the protein solution and follicular fluid. The diameter ratio of both showed the same curve up to the midpoint of the IC or VC regime, and the follicular fluid evolved further over time to reach the EC regime. These findings suggest that other components of the follicular fluid, such as peptides and cumulus cells [20–22], influence its rheological properties, even though proteins by themselves do not exhibit elastic properties. Although we could not identify significant differences in the shear viscosity data between the protein solution and follicular fluid (Figure 6), the aforementioned findings would not have been known without performing extensional viscometry.

For each diameter ratio data (Figure 10A), a graph organized with the time reference as the onset time of the EC regime t_{EC} is shown in Figure 10B. For Newtonian fluids such as pure water and protein solutions, t_{EC} is considered the breakup time of the liquid filament. We found that the slope of the diameter ratio graph in the EC regime of the follicular fluid was in relatively good agreement with that of the PEO solution at a concentration of 0.05 wt%. The relaxation times of the dilute polymer solutions in the EC regime and follicular fluid were calculated using Eq. 1. The relaxation times of the dilute polymer solutions were $\lambda_E = 1.18, 0.36,$ and 0.11 ms for the concentrations of 0.1, 0.05, and 0.03 wt%, respectively, while that of the follicular fluid was $\lambda_E = 0.37$ ms. Therefore, the extensional viscosities and relaxation times of 0.05 wt% PEO solution ($\lambda_E =$

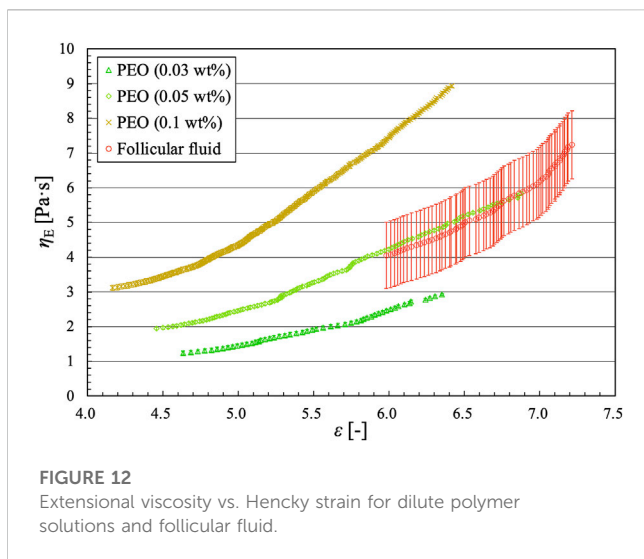


FIGURE 12
Extensional viscosity vs. Hencky strain for dilute polymer solutions and follicular fluid.

0.36 ms) and follicular fluid ($\lambda_E = 0.37$ ms) are similar, suggesting that they are viscoelastic fluids with similar extensional behavior.

Next, the extension rate (or strain rate) was derived to investigate the reliability of t_{EC} . To determine whether the extensional behavior of complex fluids in the EC regime is uniaxial extensional flow, Hencky strain ϵ was introduced and expressed in the following equation as the length of the liquid filament that is deformed from L_0 to L (Figure 4B):

$$\epsilon = \ln\left(\frac{L}{L_0}\right) = \ln\left(\frac{D_0}{D}\right)^2 = 2 \ln\left(\frac{D_0}{D}\right) \quad (2)$$

As the extension rate is theoretically constant in the EC regime [27], the latter was determined from the time variation graph of the extension rate calculated from the diameter ratio data. The extension rate $\dot{\epsilon}$ is the derivative in the Hencky strain ϵ with time t , and is expressed from the diameter ratio of the liquid filament D/D_0 as follows:

$$\dot{\epsilon} = -2 \frac{d \ln(D/D_0)}{dt} = -\frac{2}{D} \frac{dD}{dt} \quad (3)$$

Figure 11 shows the time variation in the extension rate in 0.05 wt% PEO solution and follicular fluid. In the dilute polymer solution, there was an inflection point at time when the extension rate increased/decreased (at $t - t_{EC} = -0.04$ ms), after which it became constant. Generally, this inflection point exists at the end of the IC or VC regime for viscoelastic fluids, and the time at which the extension rate reaches a constant value after decreasing is known to be the onset of the EC regime [27]. The time range of the EC regime $t - t_{EC}$ in the dilute polymer solution was set between 0 and 1.09 ms, and the Hencky strain ϵ varied between 4.46 and 6.88. In the case of follicular fluid, the variation in the extension rate was gentle, and there was an inflection point where the extension rate slightly increased/decreased (around $t - t_{EC} = -0.5$ ms), after which it was observed to be constant. Therefore, we determined that the time range of the EC regime $t - t_{EC}$ was between 0 and 0.65 ms, and the Hencky strain ϵ was estimated to be between 5.98 and 7.21. When deriving the extensional viscosity, it is necessary to assume that the liquid filament is cylindrical in the EC regime and that the extensional stress σ_E acting on the filament is only the pressure

difference Δp ; thus, the extensional viscosity η_E is expressed as follows:

$$\eta_E = \frac{\sigma_E}{\dot{\epsilon}} = \frac{\Delta p}{\dot{\epsilon}} = \frac{2\Gamma}{\dot{\epsilon}D} = -\frac{\Gamma}{dD/dt} \quad (4)$$

where Γ is the surface tension of the liquid. The surface tension of the follicular fluid was measured in 10 trials using the Wilhelmy plate method (DY-300, Kyowa Interface Science Co. Ltd.), and the average value was $\Gamma = 52.4 \pm 0.4$ mN/m. Figure 12 shows the extensional viscosity η_E plotted against the Hencky strain ϵ for dilute polymer solutions and follicular fluid. For the former, the extensional viscosity increased monotonically with increasing Hencky strain, thereby expanding the range of extensional viscosity. Both the Hencky strain range and extensional viscosity increased with increasing solution concentration. This was because the slope of the diameter ratio in the EC regime decreased with increasing solution concentration, and the diameter ratio increased around the transition time ($t = t_{EC}$) from the IC or VC regime to the EC regime (Figure 10B). This trend was confirmed in a previous study using the same concentrations of PEO solutions [26]. For the follicular fluid, the range of the Hencky strain in the EC regime was smaller than that for the dilute polymer solutions. The extensional viscosity η_E of follicular fluid was estimated to be between 4.0 and 7.2 Pa s, and almost the same as that of the PEO solution (0.05 wt%), which suggests that the rheological property of the follicular fluid is comparable to that of 0.05 wt% PEO solution.

4 Conclusion

This study aimed to examine the rheology of human follicular fluids in terms of shear and extensional viscosities, and compare it to that of pure water, protein solutions, and dilute polymer solutions at three distinct concentrations. Despite the alteration in the color of the follicular fluid due to RBC removal via centrifugation, no discernible modification was observed in its shear viscosity. Moreover, the shear viscosity of follicular fluid remained constant even when the stress loading time increased. A comparison between the shear viscosities of follicular fluids that contained oocytes and those that did not revealed a marked difference that may be attributable to the distinct components, such as proteins and peptides, of follicular fluid, warranting further investigation of the causal relation. These findings suggest that the presence of oocytes in follicular fluids can be inferred from their shear viscosities, even if the present measurements were not conducted *in situ*. Moreover, an extensional viscosity measurement system based on the liquid dripping approach was designed and used to measure a sample volume of less than 3 mL. Pure water and OVA solution did not exhibit axial extension, whereas PEO solutions and follicular fluid exhibited extensional behavior. The diameter ratio curves for pure water and PEO solutions in the IC/VC regime closely resembled those for OVA solution and follicular fluid, respectively. However, upon comparing the diameter ratio curves of the protein solution and follicular fluid, only the latter was revealed to possess an EC regime. Therefore, OVA is not the sole determinant of the rheological properties of follicular fluid. Additionally, the extensional viscosity of follicular fluid was directly proportional to the Hencky strain, displaying a similar trend to that observed in dilute polymer solutions.

The extensional viscosity characteristics of follicular fluid showed high sample variability and were comparable to those of low-viscosity dilute polymer solutions, making the measurement of extensional viscosity of the fluid itself highly challenging. Hence, it is difficult to determine the developmental stage of oocytes based on differences in the extensional viscosity characteristics of follicular fluid. To establish such a relation, the development of an extensional viscosity measurement technique specifically for measuring lower viscosity solutions and investigation of the extensional viscosity of a large number of follicular fluid samples should be conducted in the future.

Data availability statement

The original contributions presented in the study are included in the article/[Supplementary Materials](#), further inquiries can be directed to the corresponding author.

Ethics statement

The studies involving humans were approved by the Bioethical review committees of Nagoya Institute of Technology (approval no. 2022-7) and Bioethical review committees of Nagoya University Hospital (approval no. 2022-0010). The studies were conducted in accordance with the local legislation and institutional requirements. The participants provided their written informed consent to participate in this study.

Author contributions

MM: Conceptualization, Funding acquisition, Investigation, Project administration, Resources, Writing–original draft, Writing–review and editing, Visualization, Supervision, Methodology. KK: Data curation, Formal Analysis, Investigation, Methodology, Visualization, Writing–review and editing. TY: Data curation, Formal Analysis, Investigation, Methodology, Visualization, Writing–review and editing. AM: Conceptualization, Resources, Visualization, Writing–review and editing. SI: Conceptualization, Resources, Writing–review and editing, Methodology. MN: Conceptualization, Resources, Writing–review and editing, Investigation, Methodology. SO:

Conceptualization, Resources, Visualization, Writing–review and editing. ST: Conceptualization, Funding acquisition, Methodology, Project administration, Resources, Supervision, Visualization, Writing–original draft, Writing–review and editing.

Funding

The author(s) declare financial support was received for the research, authorship, and/or publication of this article. The research conducted in this study was financially supported by the Nitto Foundation.

Acknowledgments

We express our gratitude to Haruki Yamamoto, Kaya Miyata, and Sho Akeda for performing the measurements.

Conflict of interest

The authors declare that the research was conducted in the absence of any commercial or financial relationships that could be construed as a potential conflict of interest.

Publisher's note

All claims expressed in this article are solely those of the authors and do not necessarily represent those of their affiliated organizations, or those of the publisher, the editors and the reviewers. Any product that may be evaluated in this article, or claim that may be made by its manufacturer, is not guaranteed or endorsed by the publisher.

Supplementary material

The Supplementary Material for this article can be found online at: <https://www.frontiersin.org/articles/10.3389/fphy.2023.1308322/full#supplementary-material>

References

- Chambers GM, Dyer S, Zegers-Hochschild F, de Mouzon J, Ishihara O, Banker M, et al. International committee for monitoring assisted reproductive technologies world report: assisted reproductive technology, 2014. *Hum Reprod* (2021) 36:2921–34. doi:10.1093/humrep/deab198
- Tierney K The future of assisted reproductive technology live births in the United States. *Popul Res Pol Rev* (2022) 41:2289–309. doi:10.1007/s11113-022-09731-5
- Katagiri Y, Jwa SC, Kuwahara A, Iwasa T, Ono M, Kato K, et al. Assisted reproductive technology in Japan: a summary report for 2020 by the ethics committee of the Japan Society of obstetrics and gynecology. *Reprod Med Biol* (2023) 22:e12494. doi:10.1002/rmb2.12494
- McDowell S, Kroon B, Ford E, Hook Y, Glujovsky D, Yazdani A. Advanced sperm selection techniques for assisted reproduction. *Cochrane Database Syst Rev* (2014) 10:CD010461. doi:10.1002/14651858.CD010461.pub2
- Swann K. The role of Ca²⁺ in oocyte activation during *in vitro* fertilization: insights into potential therapies for rescuing failed fertilization. *Biochim Biophys Acta Mol Cel Res* (2018) 1865:1830–7. doi:10.1016/j.bbamcr.2018.05.003
- Salih M, Austin C, Warty RR, Tiktin S, Rolnik DL, Momeni M, et al. Embryo selection through artificial intelligence versus embryologists: a systematic review. *Hum Reprod Open* (2023) 2023:hoad031. doi:10.1093/hropen/hoad031
- Practice Committees of the American Society for Reproductive Medicine and the Society for Assisted Reproductive Technology. The use of preimplantation genetic testing for aneuploidy (PGT-A): a committee opinion. *Fertil Steril* (2018) 109:429–36. doi:10.1016/j.fertnstert.2018.01.002
- Young JM, McNeilly AS. Theca: the forgotten cell of the ovarian follicle. *Reproduction* (2010) 140:489–504. doi:10.1530/REP-10-0094

9. Gosden RG, Hunter RH, Telfer E, Torrance C, Brown N. Physiological factors underlying the formation of ovarian follicular fluid. *J Reprod Fertil* (1988) 82:813–25. doi:10.1530/jrf.0.0820813
10. Dumesic DA, Meldrum DR, Katz-Jaffe MG, Krisher RL, Schoolcraft WB. Oocyte environment: follicular fluid and cumulus cells are critical for oocyte health. *Fertil Steril* (2015) 103:303–16. doi:10.1016/j.fertnstert.2014.11.015
11. Dumesic DA, Abbott DH. Implications of polycystic ovary syndrome on oocyte development. *Semin Reprod Med* (2008) 26:053–61. doi:10.1055/s-2007-992925
12. Meng Q, Polgar Z, Tancos Z, Tian X, Dinnyes A. Cloning of rabbits. In: Cibelli J, Gurdon J, Wilmut I, Jaenisch R, Lanza R, West MD. *Principles of cloning*. Cambridge: Academic Press (2014). p. 227–44.
13. Lenton EA, King H, Thomas EJ, Smith SK, McLachlan RI, MacNeil S, et al. The endocrine environment of the human oocyte. *J Reprod Fertil* (1988) 82:827–41. doi:10.1530/jrf.0.0820827
14. Basuino L, Silveira CF, Jr. Human follicular fluid and effects on reproduction. *JBRA Assist Reprod* (2016) 20:38–40. doi:10.5935/1518-0557.20160009
15. Luck MR, Ye J, Almslimani H, Hibberd S. Follicular fluid rheology and the duration of the ovulatory process. *J Reprod Fertil* (2000) 120:411–21. doi:10.1530/jrf.0.1200411
16. Fisch B, Harel L, Amit S, Kaplan-Kraicer R, Mor N, Tadir Y, et al. Viscosity and refractive index of follicular fluid in relation to *in vitro* fertilization. *J Assist Reprod Genet* (1996) 13:468–71. doi:10.1007/BF02066526
17. Kolbasov A, Comiskey PM, Sahu RP, Sinha-Ray S, Yarin AL, Sikarwar BS, et al. Blood rheology in shear and uniaxial elongation. *Rheol Acta* (2016) 55:901–8. doi:10.1007/s00397-016-0964-1
18. Pritchard MF, Powell LC, Menzies GE, Lewis PD, Hawkins K, Wright C, et al. A new class of safe oligosaccharide polymer therapy to modify the mucus barrier of chronic respiratory disease. *Mol Pharm* (2016) 13:863–72. doi:10.1021/acs.molpharmaceut.5b00794
19. Bazilevsky AV, Entov VM, Rozhkov AN. Breakup of a liquid bridge as a method of rheological testing of biological fluids. *Fluid Dyn* (2011) 46:613–22. doi:10.1134/S0015462811040119
20. Bayasula IA, Kobayashi H, Goto M, Nakahara T, Nakamura T, et al. A proteomic analysis of human follicular fluid: comparison between fertilized oocytes and non-fertilized oocytes in the same patient. *J Assist Reprod Genet* (2013) 30:1231–8. doi:10.1007/s10815-013-0004-3
21. Shen X, Liu X, Zhu P, Zhang Y, Wang J, Wang Y, et al. Proteomic analysis of human follicular fluid associated with successful *in vitro* fertilization. *Reprod Biol Endocrinol* (2017) 15:58. doi:10.1186/s12958-017-0277-y
22. Shalgi R, Kraicer P, Rimon A, Pinto M, Soferman N. Proteins of human follicular fluid: the blood-follicle barrier. *Fertil Steril* (1973) 24:429–34. doi:10.1016/S0015-0282(16)39730-8
23. Dinic J, Biagioli M, Sharma V. Pinch-off dynamics and extensional relaxation times of intrinsically semi-dilute polymer solutions characterized by dripping-onto-substrate rheometry. *J Polym Sci B Polym Phys* (2017) 55:1692–704. doi:10.1002/polb.24388
24. Tamano S, Bunya A. Comparison of rheological properties between DoS and liquid dropping methods in uniaxial extensional flow of dilute polymer aqueous solutions [Article in Japanese]. *Nihon Reorji Gakkaishi* (2022) 50:363–70. doi:10.1678/rheology.50.363
25. Tirtaatmadja V, McKinley GH, Cooper-White JJ. Drop formation and breakup of low viscosity elastic fluids: effects of molecular weight and concentration. *Phys Fluids* (2006) 18:043101. doi:10.1063/1.2190469
26. Dinic J, Zhang Y, Jimenez LN, Sharma V. Extensional relaxation times of dilute, aqueous polymer solutions. *ACS Macro Lett* (2015) 4:804–8. doi:10.1021/acsmacrolett.5b00393
27. Dinic J, Sharma V. Flexibility, extensibility, and ratio of Kuhn length to packing length govern the pinching dynamics, coil-stretch transition, and rheology of polymer solutions. *Macromolecules* (2020) 53:4821–35. doi:10.1021/acs.macromol.0c00076
28. Nashima T. Development of a sensitive Couette rheometer [Article in Japanese]. *Nihon Reorji Gakkaishi* (2007) 35:179–83. doi:10.1678/rheology.35.179
29. Takeshi N. Improvement of a sensitive coaxial-cylinder rotational viscometer. *AIST Bull Metrology* (2005) 4:93–8.
30. Tamano S, Ohashi Y, Morinishi Y. Dynamics of falling droplet and elongational properties of dilute nonionic surfactant solutions with drag-reducing ability. *Phys Fluids* (2017) 29:053104. doi:10.1063/1.4984000
31. Magata F, Horiuchi M, Echizenya R, Miura R, Chiba S, Matsui M, et al. Lipopolysaccharide in ovarian follicular fluid influences the steroid production in large follicles of dairy cows. *Anim Reprod Sci* (2014) 144:6–13. doi:10.1016/j.anireprosci.2013.11.005
32. Trejo-Soto C, Hernández-Machado A. Normalization of blood viscosity according to the hematocrit and the shear rate. *Micromachines (Basel)* (2022) 13:357. doi:10.3390/mi13030357
33. Ewoldt RH, Johnston MT, Caretta LM. Experimental challenges of shear rheology: how to avoid bad data. In: Spagnolie S, editor. *Complex fluids in biological systems: experiment, theory, and computation*. New York, NY: Springer (2015). p. 207–41.
34. Castellanos MM, Pathak JA, Colby RH. Both protein adsorption and aggregation contribute to shear yielding and viscosity increase in protein solutions. *Soft Matter* (2014) 10:122–31. doi:10.1039/c3sm51994e
35. Lauser KT, Rueter AL, Calabrese MA. Small-volume extensional rheology of concentrated protein and protein-excipient solutions. *Soft Matter* (2021) 17:9624–35. doi:10.1039/d1sm01253c
36. Tammamo D, Chandran Suja V, Kannan A, Gala LD, Di Maio E, Fuller GG, et al. Flowering in bursting bubbles with viscoelastic interfaces. *Proc Natl Acad Sci* (2021) 118:e2105058118. doi:10.1073/pnas.2105058118
37. Regev O, Vandebriel S, Zussman E, Clasen C. The role of interfacial viscoelasticity in the stabilization of an electrospun jet. *Polymer* (2010) 51:2611–20. doi:10.1016/j.polymer.2010.03.061
38. Brust M, Schaefer C, Doerr R, Pan L, Garcia M, Arratia PE, et al. Rheology of human blood plasma: viscoelastic versus Newtonian behavior. *Phys Rev Lett* (2013) 110:078305. doi:10.1103/PhysRevLett.110.078305